B. Tech project report on

SELF-ASSEMBLY OF COLLOIDAL NANOPARTICLES FROM SESSILE EVAPORATING DROPS

For partial fulfillment of the requirements for the degree of

Bachelor of Technology

In

Chemical Engineering

Submitted by:

Siddharth Mahapatra

Roll Number- 109CH0116

Under the guidance of:

Dr. Santanu Paria

Department of Chemical Engineering,

National Institute of Technology,

Rourkela-769008

2013

Department of Chemical Engineering,
National Institute of Technology,
Rourkela-769008, Odisha

CERTIFICATE

This is to certify that the project report entitled "**Self-assembly of colloidal nanoparticles from sessile evaporating drops**" submitted by **Siddharth Mahapatra (109CH0116)** in partial fulfillment of the requirements for the award of degree of Bachelor of Technology in Chemical Engineering at National Institute of Technology, Rourkela is an authentic work carried out by him under my supervision and guidance.

To best of knowledge, the matter embodied in this thesis has not been submitted to any other university or institute for the award of any degree.

Date: 3/5/2013

Place: Rourkela

Dr. Santanu Paria
Department of Chemical Engineering,
National Institute of Technology,
Rourkela-769008

ACKNOWLEDGEMENT

In pursuit of this academic endeavor, I feel that I have been singularly fortunate; inspiration, guidance, direction, cooperation, love and care all came in my way in abundance and it seems almost an impossible task for me to acknowledge the same in adequate terms. Yes, I shall be failing in my duty if I do not record my profound sense of indebtedness and heartfelt gratitude to my supervisor Dr. Santanu Paria who guided and inspired me in pursuance of this work. His association will remain a beacon of light to me throughout my career.

I owe a depth of gratitude to Prof. R.K.Singh, H.O.D, Department of Chemical Engineering, for all the facilities provided during the course of my tenure.

A special thanks to my all lab mates Mr. Rohit Omar, Mr. Rajib Ghosh Chaudhuri and Mr. K. Jagajjanani Rao for making a good atmosphere in the lab. I thank Siddhant Panda for his constant help, support and insight. I am also thankful to my friends Ankit Kedia and Manas Ranjan Das for their help and support.
I thank for the support, encouragement and good wishes of my parents and family members, without which I would not have been able to complete my report.

Date: 06/05/2013

Place: Rourkela

Siddharth Mahapatra

Roll No: - 109CH0116,

Department of Chemical Engineering,

National Institute of Technology,

Rourkela-769008

TABLE OF CONTENTS

ABSTRACT

Science and technology has advanced to such extent that the size of devices and machines used for making daily work easy has reduced greatly. As such, fabrication of devices on planar surfaces is catching more attention and traditional methods have become obsolete. Fabrication at small-scale has been made easier and inexpensive by the use of a relatively novel technique called self-assembly. The present work is divided into two parts: formation of fractal self-assembly patterns from colloidal sulphur in acidic medium, and from sodium carboxymethylcellulose (CMCNa) in alkaline medium.

When droplets of colloidal suspensions are evaporated, a dense ring-like deposition is formed; a phenomenon known as coffee-ring effect. Since it takes place by the outward flow within the drop and an overall evaporative flux which causes circulation towards the centre of drop, a coffee-ring like structure is formed. According to theory, by varying the particle concentration and the alkali used, the structure morphology can be varied. In this work, formation of self-assembled structures from colloidal sulphur particles and polyelectrolyte chains of CMCNa by drying of microliter-sized droplets on glass surface has been investigated by optical microscopy. Results of this work show that tree-like branched structures are formed after evaporation of drops of the reaction mixture. Various factors influence the structure formation, such as particle concentration, alkali concentration, pH of the solution, drop volume, reaction and drying temperatures, and drying time. Theoretically, the structure formation is controlled by evaporative flux inside the liquid drop, capillary condensation, and van der Waals forces of attraction between particles. Different alkali concentrations when used for the reaction bring about change in morphology of the structures in the reaction mixture. At lower alkali concentrations, the structure was sharper with fully-formed fractal patterns, while at high concentrations, thicker floral patterns were formed. Similar acid concentration has qualitative effect on self-assembly of colloidal sulphur particles. Change of substrate can also modify the self-assembly, which will form the basis of future work. Also theoretical modeling of self-assembly can be done from known parameters.

Keywords: self-assembly, colloidal sulphur, microliter drops, CMCNa, polyelectrolyte, nanoparticles, coffee-ring effect, van der Waals force, capillary force.

LIST OF FIGURES

NOMENCLATURE

RFID	Radio Frequency Identification
UV	Ultra Violet
CVD	Chemical Vapor Deposition
pH	Potential of Hydrogen
DNA	Deoxyribonucleic acid
AFM	Atomic Force Microscopy
XRR	X-Ray Reflectometry
SEM	Scanning Electron Microscopy
XRD	X-Ray Diffraction
TEM	Transmission Electron Microscopy
DODA	Dioctadecylamine
CMCNa	Sodium carboxymethylcellulose
FTIR	Fourier Transform Infrared Spectroscopy
GCMS	Gas Chromatography Mass Spectroscopy
AVO	Acid Vapor Oxidation
DLVO	Derjaguin and Landau,Verwey and Overbeek.
DLS	Dynamic Light Scattering
OCA	Optical Contact Angle
DLA	Diffusion Limited Aggregation

LIST OF SYMBOLS

δ	Delta, difference
Ω	Ohm, Electrical resistance
ζ	Zeta potential
π	Pi, 22/7
θ	Theta, Contact angle, °
λ	Lambda, $(\pi - 2\theta)/(2\pi - 2\theta)$
g	Surface tension of the liquid
$F_{flotation}$	Lateral flotation forces
$F_{immersion}$	Lateral immersion forces
r_p	Critical particle radius
K_1	Bessel's function
q^{-1}	Characteristic length or the range of the capillary force
l	Distance between two particles
s	Seconds
d_s	Drop size
h_r	Drop height
r	Distance from the centre of the drop
d_p	Particle diameter
α_{rtd}	retardation factor for van der Waals force
β	gradient of surface tension with temperature [N m^{-1} K^{-1}]

γ	function of surface potential, surface tension [Nm^{-1}]
φ	wetting angle of the drop
ε	dielectric constant of the water [78.54]
ε_0	vacuum permittivity [$8.85x10^{-12}$ C^2 J^{-1} m^{-1}]
κ^{-1}	Debye screening length [m]
ψ	surface potential [V]
μ	dynamic viscosity [Pa s]
F	density of drop liquid [kg/m^3]
σ	surface charge density [C m^{-2}]
a	arbitrary constant
A	Hamaker constant (= 2.43 $x10^{-20}$ J for water)
C	concentration [mol/L]
d	diameter [m]
D_{pl}	diffusion coefficient of particles in liquid [m^2/s]
e	electronic unit charge [1.6x 10^{-19} C]
F	force between a particle and substrate [N], Faraday constant (96500 C/mol)
g	gravitational acceleration [9.81 m/s^2]
I	ionic strength of solution [mol/L]
k_B	Boltzmann constant [1.38 $x10^{-23}$ J K^{-1}]
m	mass of particles [kg]
n	number concentration [$molecules/m^3$]
n	unit normal vector, $n = (n_r + n_z)$
N_A	Avogadro number [6.023x 10^{23} molecules/mol]

r	radial coordinate [m]
t	time [s]
T	absolute temperature [K]
v	velocity vector, v = (u, v)
V	Volume of drop [nL], magnitude of the velocity vector v [m s^{-1}]
X	concentration of particles [kg of particles/kg of solution]
z	axial coordinate [m]

CHAPTER 1

Introduction

1. INTRODUCTION

1.1 Introduction

Self-assembly is the fundamental principle which generates structural organization on all scales, by reversible formation of structures or patterns from disordered components of a preexisting system. It may or may not require external energy and direction depending upon the thermodynamics of the system. The disordered components can be perceived as the building blocks constituting the structure. Spontaneous self-assembly can occur in nature, for instance in cells (self-assembly of the lipid bilayer membrane) and other biological systems, such as DNA, as well as in fuzzy systems, which usually results in the increase in order and organization of the system. Since the building blocks of self-assembled structure usually fall in the size range of colloidal nanoparticles, hence bottom-up approach can be used for fabrication of self-assembled structures. Different forces act at different size levels. At micron level capillary force, surface tension, and external field forces such as gravitational and electromagnetic forces play a major role, while major nano and molecular level forces acting are electrostatic forces, van der Waals interactions, hydrogen bonding and DLVO interactions. A large number of biological systems assemble various molecules and structures by self-assembly. To replicate these strategies and creating novel molecules that can self-assemble into supramolecular assemblies is an important technique in nanotechnology, with the added advantages of cost-effectiveness, versatility and the possibility of minimum defect self-healing systems.

1.2 Background

Nanotechnology is a relatively modern development in scientific research. However the development of its fundamental concepts happened over a larger period of time. Exaggerated expectations and unrealistic claims were followed by a return to basic concepts and fundamental aspects of technology. As the research started becoming more application-oriented, nanoparticles with unique properties were synthesized and their behaviour was studied. Recent trend is the formation of spontaneously organized nanostructures which opens up new possibilities in the design of nano level systems. Deegan et al. [1] gave the first report regarding formation of self-assembled structures from colloidal particles, which also

explained the ring-like formation after drying on solid surfaces akin to coffee stains. Since then self-assembly of colloidal particles has been explained by many researchers [1][2][3] from evaporating droplets. The role of DLVO and other intermolecular interactions in the formation of self-assembled structures [3][4] has also been studied. Variation of self-assembly formed via coffee-ring effect has been studied in some recent works [5][6]. Applications of micro fabrication in IT and nanoelectronics has urged advances in the manufacture of nanoscale components using techniques like extreme UV lithography, double patterning lithography, and multiple electron beam writing. Self-assembly methods provide simpler, inexpensive and eco-friendly methods of fabrication. Recent application includes the manufacture of RFID tags, with a >90% yield capability with self-assembly.

1.3 Self-assembled structure fabrication

The methods for fabrication of self-assembled nanostructures can be classified into dry methods and solution phase methods. Dry methods include those that take place in the absence of an aqueous medium, such as chemical vapor deposition [7], acidic vapor oxidation and laser ablation. Solution phase methods can be further classified into self-assembly in bulk solution and self-assembly by partial or complete adsorption of components on substrate, the latter consisting mostly of fluidic and evaporation assisted self-assembly methods. The advantages of solution phase methods are optimum yield, high degree of accuracy, high throughput, simplicity of process and highly favorable conditions for synthesis. These advantages have fuelled increasing amount of research in the field of electronics using self-assembly. On the other hand, dry methods are highly expensive, and are only important for an academic and research understanding of various mechanisms of self-assembly.

1.4 Applications

Self-assembly is an application of nanotechnology in terms of synthesis and microfabrication. Self-assembled structures are composed of colloidal nanoparticles which themselves have several unique properties due to their small size and specific crystal

structure. Self-assembly basically aggregates the different building blocks into ordered structures having enhanced properties. Applications of self-assembly can be broadly classified [8] into the following areas: construction of photonic materials from nanoparticles using crystalline grids and matrices, assembly of micron size components to fabricate microelectronic, nanowires and nanocircuits for robotic applications, and three-dimensional microelectronic devices [9][10].

CHAPTER 2

Background Literature

2. BACKGROUND LITERATURE

2.1 Introduction

Classification of self-assembly of nano and colloidal particles can be done into dry methods, and liquid phase methods. Major dry methods are chemical vapour deposition (CVD) [11] [12], and laser ablation. Liquid phase self-assembly methods are reclassified into (i) bulk media methods [13], and (ii) solid surface methods [1][5][14]. Solid surface self-assembly can occur by surface adsorption of particles [2][12], or by evaporation of liquid drop [1][3][4]. Aggressive procedures such as extreme UV lithographic techniques, focused-ion beam, electron beam etc. have been used till recently for creating nanostructures on metal and polymer substrates. However dry processes such as CVD and laser ablation have no scope for mass manufacture and the yield is very low. Self-assembly has attracted more attention as the whole process is autonomous and one has full control over the reaction parameters such as pH, temperature and addition of organic molecules which allows creation of several different fascinating structures. Moreover there is no need of external supervision as the building blocks generated by precursors spontaneously self-assemble into thermodynamically stable structures.

2.2 Classification of Self-assembly processes

As discussed earlier, self-assembly methods can be broadly classified into dry methods and solution-phase methods. Solution-phase methods are again sub-divided based on the components involved in the self-assembled structure. Some of these components are particles, nanocrystals, and polymers. Particles or nanoparticles are formed from precipitation reaction and possess intermolecular interaction in the solvent. Nanocrystals are also synthesized similarly with the addition being the use of organic reagents for crystal surface modification allowing different types of crystal growth from same precursors. Polymers exhibit multiple unique patterns also.

Banerjee et.al. [2] describes a drying-mediated process of forming self-assembled monolayers of thiol-capped gold nanocrystals. In their process dodecanethiol

capped gold particles were suspended in toluene and then spread on a Langmuir trough. Hydrophobicity of the particles enables them to float on the water surface, and after evaporation of the solvent a monolayer is formed at the air-water interface, which is studied by AFM and XRR techniques. The pattern formation was found to increase with increase in surface-pressure during adsorption. Due to spreading in the Langmuir trough, some of the particles coalesce driven by kinetic self-assembly, and the monolayer formation on the substrate causes the particles to come closer by drying process and intermolecular forces.

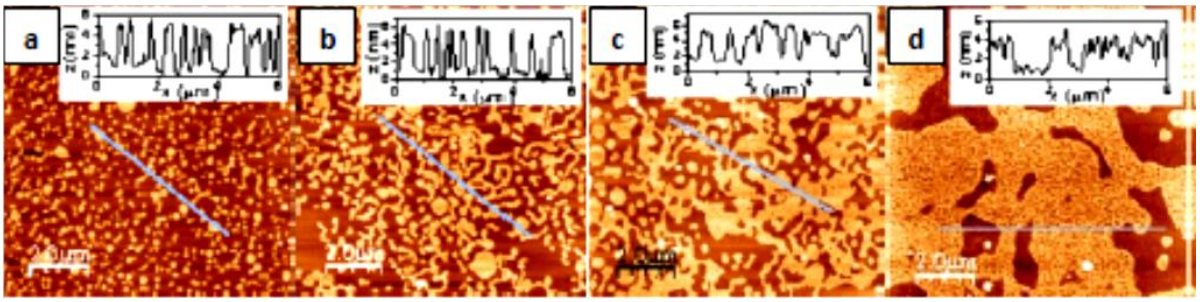

Figure 1 Nanopattern formation in self assembled monolayers of thio-capped Au nanocrystals [2]

Another theory says that pattern formation is caused by the drying of water from the surface in definite pathways which can be attributed to hydrodynamic convection currents (Bernard-Marangoni convection). John et.al. [15] also synthesized the above described nanocrystals and their work describes formation of cellular networks and a form of programmed self-assembly achieved by capping nanoparticles with molecules and ligands that can self-assemble, such as alkanethiols and alkylamines. They also explain the appearance of water as centers of nucleation and growth for agglomerates and clusters, by AFM studies. Water introduced gets absorbed on the hydrophilic mica surface forming monolayers and microdomains, which grow to form domains and the particles, are able to diffuse better. This explains the cause of self-assembly in a clearer manner. Surfactants also play a major role in self-assembly, of restricting further growth by surface adsorption. Self-assembly of nanocrystals of metals, metal oxides, sulfides and other semiconductor materials has been studied recently [12]. XRD, SEM and TEM images show that there is tendency for self-assembly to occur by sharing of the planar faces of the crystals. Jun et.al. [16] attempted to explain the processes guiding the shapes of various morphologies for nanocrystals, such as rods, spheres, cubes, disks, etc. Various factors contribute in the formation of different morphologies, such as crystalline phase of the nucleates, surface energy, kinetic and thermodynamic growth and selective adsorption of capping ligands.

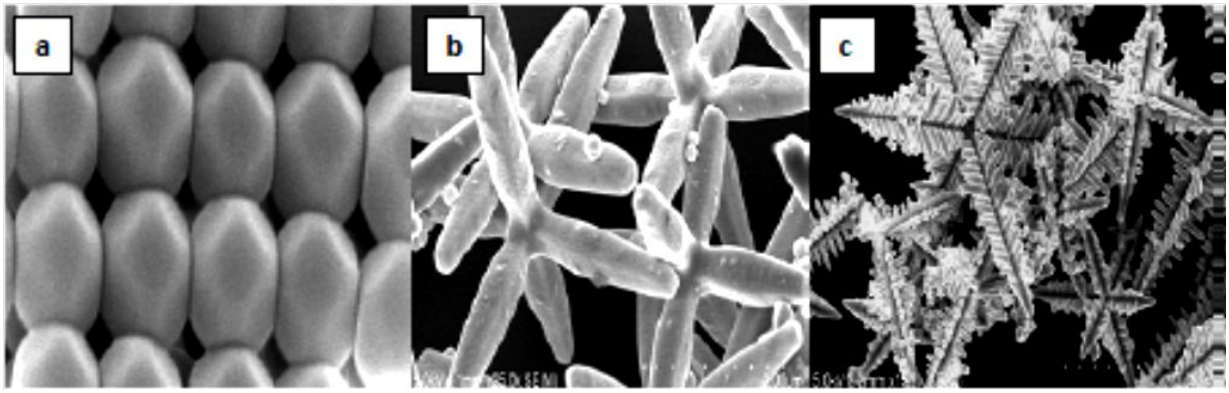

Figure 2 Synthesis of PbS truncated octahedron crystals with high symmetry into different structures [12]

Self-assembly of colloidal particles is by far the simplest, energy effective and cost effective process for fabrication of self-assembled nanostructures. It can be carried from all varieties of particles including those that are synthesized within the reaction media using the particle solution and substrate for self-assembly. Deegan et.al. [1]'s work regarding ring like patterns formed from drying liquid drops, has made this method popular. According to their work, capillary forces hold the particles together at the periphery of the drop,

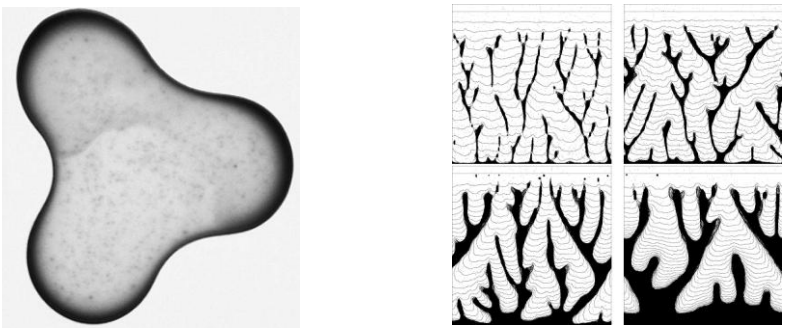

Figure 3 The "coffee ring" effect and variation of structure with particle concentration [1][19]

where there is maximum effect of the force due to low liquid height and high particle concentration. Presence of salt/solute causes Marangoni flow currents, which complement for the fluid lost in evaporation and hence flow oppositely to the fluid, to take place. Some studies [17][18] have explained the effect of capillary forces between particles, size dependent segregation of particles and formation of organized 2D arrays of particles. Vancea et.al. [19] simulates various conditions of pattern formation. Their study shows that the final structure attributes to the changes in particle concentration and particle mobility within

solution. Presence of unstable “fingering” patterns cause the formation of branch and leaf-like structures, which is indicative of the Mullins-Sekerka instability occurring due to presence of salts in particle solution. Parameters such as particle size and concentration, which affects the interparticle interaction, and the substrate, ultimately decide the final structure.

Semi-crystalline polymers have also been employed in the preparation of self-assembled monolayers. Recent studies have been done on amphiphilic molecules such as DODA (dioctadecylamine), EP (ethyl palmitate), ES (ethyl stearate), etc. Observations show that these monolayers exhibit crystal morphologies such as dendrites and fractal structures. Preparation often involves spreading polymer solution into thin films in Langmuir trough, or spin-casting of polymer solution onto substrate. The main cause of various crystal morphologies is diffusion-limited crystal growth. Decreasing film thickness drastically affects the molecular mobility, glass transition temperature and segmental orientation of semi-crystalline polymers, which ultimately affects the self-assembly structure.

2.3 Research objective

Self-assembly easily stands out as the simplest, most efficient and highest yielding method of structure fabrication and surface modification. It also requires minimal human intervention, hence having the unique attribute of automaticity. In this work, the formation of self-assembled patterns using colloidal sulfur particles from specific reactions (synthesized in-situ) on glass surfaces has been studied. Structure formation of sulfur solutions synthesized from oxalic acid, HCl and H_2SO_4 have been studied. Primary objectives of the project are:

i. To gain an insight into the mechanism of evaporation-induced self-assembled structure formation using colloidal sulfur on flat surfaces.
ii. To study the effect of various acids on the morphology of the self-assembled patterns.

This method of synthesizing colloidal particles in the reaction media and using the reaction solution to generate self-assembled structures on flat surfaces is a simple and novel process and these factors provide motivation for the project.

CHAPTER 3

SELF-ASSEMBLY OF COLLOIDAL SULFUR PARTICLES ON GLASS SURFACE FROM EVAPORATING DROPS

3. SELF-ASSEMBLY OF COLLOIDAL SULFUR PARTICLES ON GLASS SURFACE FROM EVAPORATING DROPS

3.1 Introduction

Self-assembly is the process by which colloidal particles, nanoparticles, or macromolecules follow a thermodynamically stable organized arrangement, by the effect of various favorable forces. The mobile components that orient into a predictable and organized structure must be present in the desired conditions necessary to induce the required self-assembly. When the structure is stable there must be net attractive forces; an example of bottom-up approach. The novelty of this study is the formation of evaporation-induced self-assembled pattern which is also largely modified by crystallization phenomena. Self-assembly has been achieved using colloidal sulfur and the associated sodium oxalate derived from the reaction solution, by evaporation of drops of the solution on a glass surface. Effect of addition of a micron-sized substance such as kaolin (clay) has also been studied. Also other acids are used (HCl, H_2SO_4) which precipitate their respective salts in the solution (NaCl, Na_2SO_4) and modify the overall self-assembled pattern. The various driving forces responsible for the structure have also been explained by mathematical equations. It was found that the resultant complex fractal tree-like structure, is heavily dependent on the salt used, i.e., acid used, and the concentration of structures is maximum at the periphery of the dried drop.

3.2 Materials and Methods

Chemicals used in this experiment were: sodium thiosulphate ($Na_2S_2O_3$) 99% purity, oxalic acid ($H_2C_2O_4.H_2O$) 99% purity, sulphuric acid (H_2SO_4) 98% purity, hydrochloric acid (HCl) 35% purity, all from Merck India, and clay (kaolin). Some of the apparatus used were glass slides, ultrasonic homogenizer and IR lamp. Ultrapure water having resistivity 18 MΩ cm and pH 6.4-6.5 was used for all experiments.

Sulphur nanoparticles in aqueous media were prepared according to the ratios of the reactants as given in subsequent sections. Stock solution of sodium thiosulphate was prepared by dissolution of solid thiosulphate crystals in ultrapure water and acid solutions of

required concentrations were prepared from stock solution. The disproportionation reactions resulting in the formation of colloidal sulphur in acidic solutions are given as:

$$Na_2S_2O_3 + H_2C_2O_4.H_2O \longrightarrow Na_2C_2O_4 + SO_2 + S\downarrow + H_2O$$
$$Na_2S_2O_3 + 2HCl \longrightarrow 2NaCl + SO_2 + S\downarrow + H_2O$$
$$Na_2S_2O_3 + H_2SO_4 \longrightarrow Na_2SO_4 + SO_2 + S\downarrow + H_2O$$
$$SO_2 + H_2O \longrightarrow H_2SO_3$$

Constant ambient temperature of 30^0C was maintained in all the experiments. Glass slides were initially washed with methanol to remove dirt and stains and then with deionized water and dried in hot air oven to remove existent moisture. Precursors were mixed and kept for 40 min to achieve reaction equilibrium. In case of inorganic acids, the equilibrium time was 20 min. Then the suspension was sonicated in an ultrasonic equipment to break agglomerates, and prepared for observation. Microliter drops of the suspension were put on glass slides using micropipette or micro-syringe, then the slides were dried using IR lamp. The resulting dried drops were observed under an optical microscope (Hund, D600). Due to time constraints and technical difficulties, SEM and AFM analysis could not be performed.

3.3 Results and discussion

3.3.1 Observation of self-assembly

Self-assembled structures of colloidal or nano-range sulphur particles on hydrophilic glass surface after drying of small drops were studied. Optical microscope (Hund, 600 model) was used for studying the self-assembly. It was assumed that the ambient temperature remained constant when colloidal sulphur was dropped after completion of reaction, as it might affect the structure formation. Sulphur nanoparticles synthesized in organic acid catalyzed aqueous media, used in this study are mainly hydrophobic in nature and have an orthorhombic structure*.

Separate experiments were also performed with colloidal particles of kaolin and coffee added to the reaction mixture to study the effect of size in formation of self-assembled structures. Kaolin concentrations of 0.05 wt% and 0.1 wt% were used. Coffee powder was added in very low weight concentrations and the coffee-ring structure formed after drying was studied.

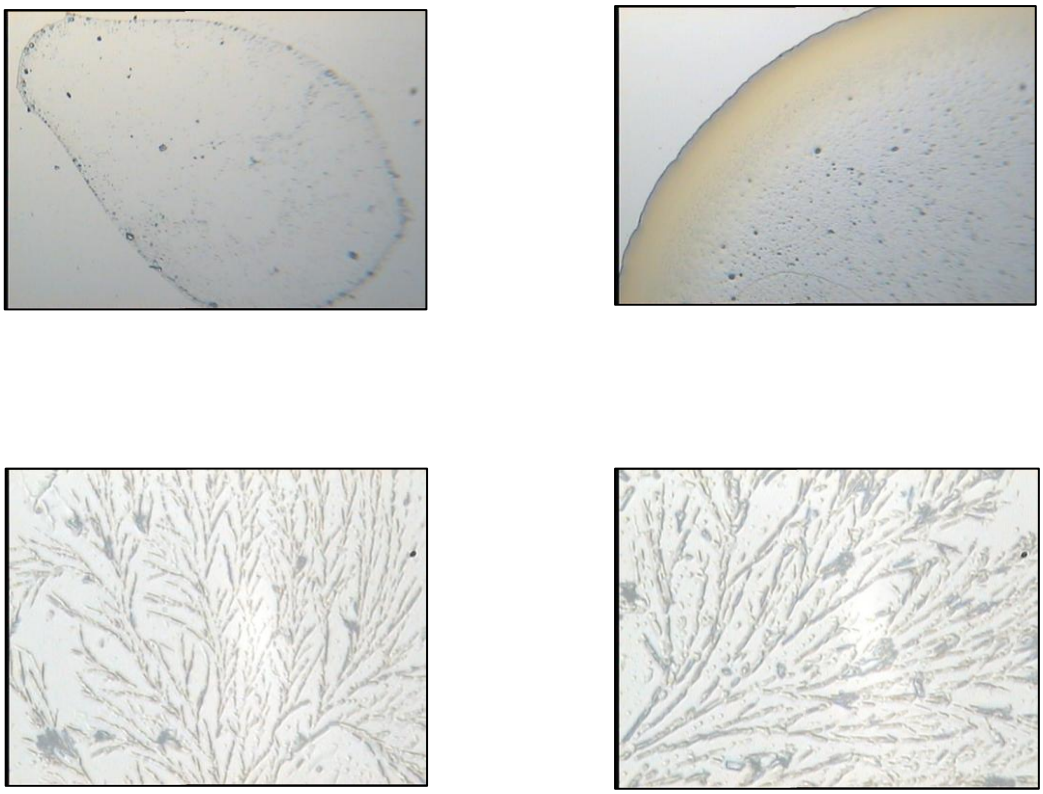

Figure 4 (clockwise from top left) Coffee ring structure, Self-assembly from coffee powder solution, Self-assembly with 0.05 wt% kaolin, Self-assembly with 0.1% kaolin.

Optical microscopy images of the pure colloidal sulfur self-assembly containing sulphur and sodium oxalate crystals are shown below:

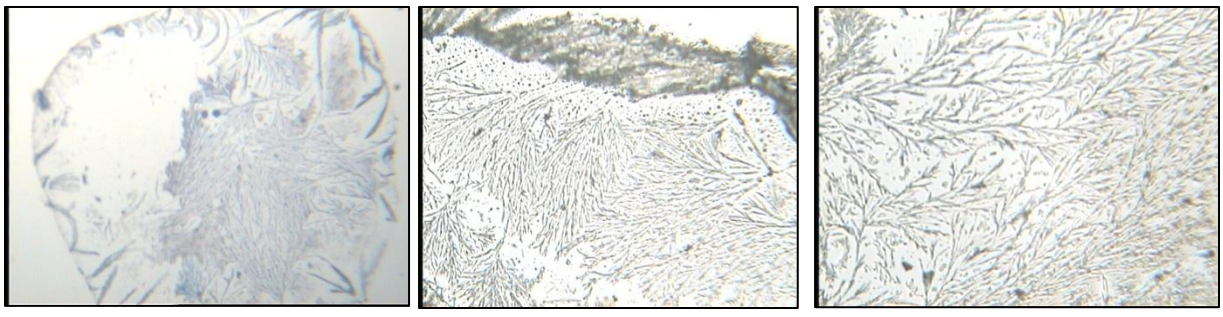

Figure 5 (left to right) Self-assembly of sulphur using 10mM conc.: Coffee-ring structure image, At 4x magnification, At 10x magnification

When other acids, such as HCl and H_2SO_4 were used instead of oxalic acid, the self-assembled structures had a labyrinthine structure and rougher edges, respectively, as compared to the tree-like fractals in the case of oxalic acid.

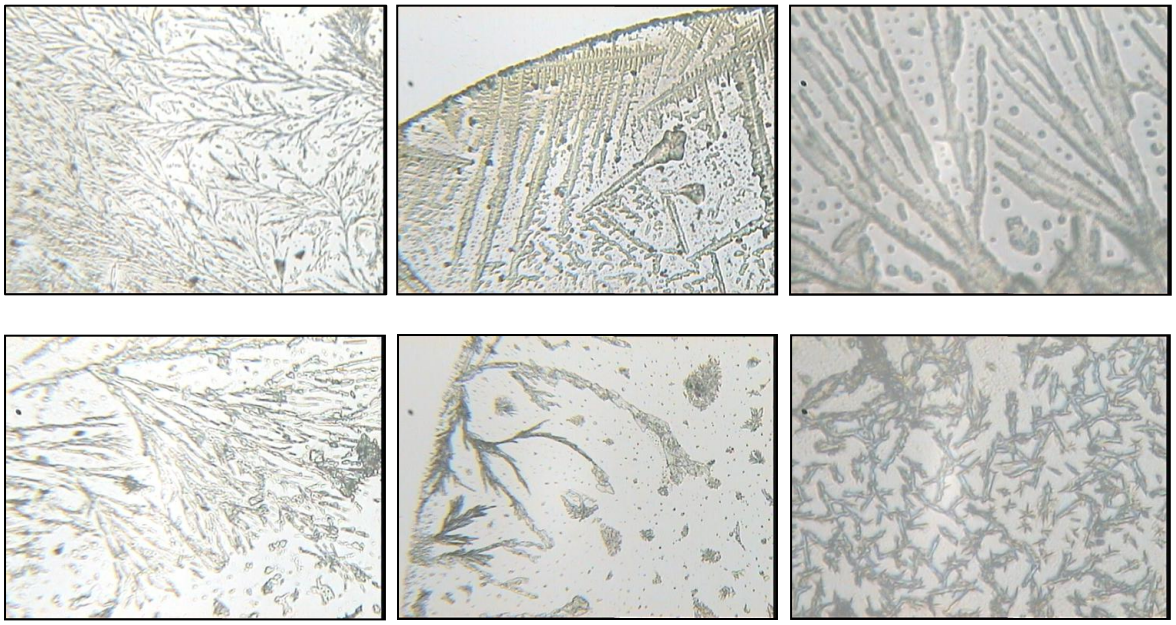

Figure 6 (clockwise from top-left) Self-assembled structures of colloidal sulphur particles from: Oxalic acid, HCl, H_2SO_4, H_2SO_4 + oxalic acid, HCl + oxalic acid, Kaolin + oxalic acid; using 10mM sulphur concentration.

3.3.2 Self-assembly of sulphur in the presence of sodium oxalate

The structures presented here are an example of dendritic crystallization due to the presence of the crystallizable salt and the colloidal sulfur particles hence the structures formed here also follow a natural fractal pattern, under the combined influence of coffee-ring effect and Marangoni flows. The fractal designs have been attributed to diffusion-limited aggregation (DLA) [20][21] in most of the previous works. They are unique apart from the basic structure the branches would follow depending on the unit cell of salt crystal. Fractal structures formed by DLA generally lack directional characteristics and the branches grow randomly, which could be due to the 'random-walking' particles which attach themselves to already immobilized particles. It is evident from the images that the structures tend to grow from the perimeter towards the center of the drop and are quite organized, which can be caused by DLA. When a liquid drop evaporates from a flat surface, there is a higher rate of

evaporation at the edge of drop gradually decreasing towards the centre of the drop, which creates a concentration gradient from the circumference to the center. Since there is higher concentration at the edges, this causes diffusive flow from the edge towards the center, i.e. Marangoni recirculation flow. Some plausible explanations that have been cited in previous works [19], are the formation of instabilities, such as Mullins-Sekerka instability [22]. Sulphur nanoparticles used here act as heterogeneous nucleation centers for crystallization of sodium oxalate in the solution, and as building blocks for the structure formation. The Marangoni effect in combination with evaporative flux, generate convection currents inside the liquid drop, which causes the particles to be in motion for as long as possible and spontaneous deposition at drop edge doesn't occur. However the attractive capillary forces and hydrophobic van der Waals force intend to cause immobilization. When a tiny liquid drop rests on a flat surface with a non-zero contact angle, the drop height gradually decreases towards the edges. At the perimeter or three phase contact line, the thin layer of liquid evaporates faster and tends to shrink the drop radius, however outward liquid flow will prevent the shrinkage of contact line up to a certain extent if the contact line of the drop contains adequate concentration of particles. Due to coffee-ring effect, the central region remains empty while structure formation takes place near the periphery. As the contact angle approaches zero due to gradual evaporation, Mullins-Sekerka instability causes dendritic crystallization to occur, which is again accelerated as colloidal sulfur acts as nucleation site for heterogeneous nucleation. During evaporation, the evaporating flux can be formulated as [1]:

$$\boldsymbol{J(r) \propto (R-r)^{-\lambda}} \qquad \textbf{(1)}$$

, where R = drop radius, r = distance from centre of drop, $\lambda = \frac{\boldsymbol{\pi - 2\theta}}{\boldsymbol{2(\pi - \theta)}}$, θ = contact angle.

Value of λ is maximum (=0.5) at zero contact angle and gradually decreases with increase in contact angle, and with increase in contact angle evaporative flux gradually increases. Initially the finer particles are transported to the contact line where they accumulate, and consequently the liquid film continuously gets thinned by evaporation. They get covered with a thin liquid layer, more of a concave film, and experience an attractive capillary force. Capillary force can be classified into two types respectively [17][18]: floatation or immersion, depending upon the respective condition of the particles. They can be represented as:

$$F_{floatation} = \frac{r_p^6}{\gamma} K_1(ql) \quad (2)$$

$$F_{immersion} = \gamma r_p^2 K_1(ql) \quad (3)$$

, where γ = surface tension of liquid, l = distance between particles, q^{-1} = range of capillary force/characteristic length, and K_1 = modified Bessel's function. Since particle size ≈ 5μm, it can be safely assumed that the attraction between particles can be attributed to $F_{immersion}$. Also when the immersion capillary force brings the particles to a close distance, van der Waals force also becomes predominant due to the hydrophobicity of the particles, which results in them getting arranged in a systematic manner to form the self-assembly. Initially, most of the particles move and deposit at the drop periphery and generate a larger diameter base of the stem. As time passes and more evaporation occurs, the smaller particles attach on the large stems and form a thinner stem growing towards the centre forming a finer structure. As particle concentration is not that high, all the particles get deposited near the edges and central region becomes vacant. From previous works, we get to know that an acid to thiosulphate ratio of 1:3 is the optimal concentration for formation of fine tree-like structures. Since the second ionization constant of the dibasic oxalic acid is low, the requirement of acid is more than the actual stoichiometric ratio of 1:1 reported above [23].

3.3.3 Effect of other acids and their respective salts on self-assembly

The formation of the structure in the presence of different salts is a complex interplay of the flow due to the differential evaporative flux, the Marangoni effect and dendritic crystallization. The Marangoni effect gradually gives way to the Mullins-Sekerka instability which causes stems of the structure to grow along the perimeter, towards the center from the high end of the concentration gradient (in terms of salt and particle concentration) of the drop. The flow due to evaporative flux tends to carry the salt and particles in the opposite direction, towards the perimeter of the drop. The maximum instability is at the edges and corners of the crystal as these are the areas with the highest surface energy, therefore the crystal growth is fastest there. Additionally, it is believed that the competition between the two flows may induce sideways branching along the high energy edges of the crystals in the previously formed stems, instead of aiding more stem growth. Ordinarily this branching wouldn't be observed for a pure salt solution. But the presences of sulfur particles which come and attach to the edges of the crystals promote nucleation and branching and further

growth of the crystal structure. This makes it clear why the structures observed in case of NaCl solutions always have branches and stems at roughly 90° to each other. It is suspected that sodium-sulphate, the salt obtained for the sulfuric acid-thio reaction has a monoclinic crystal structure in its decahydrate form (the form most likely obtained in the reaction). So this might be why we have a dendrite structure which is more crystalline as compared to the oxalic-thio structures. Sodium oxalate has an organic part in the salt, this might also be a reason why the tree structure is more of a curvy nature and comparatively less crystalline as compared to the strongly crystalline nature of the other two salts. It is also speculated that if crystal growth occurs along the different angled edges of the monoclinic unit celled sodium-sulfate crystal, the resulting structure would indeed resemble a tree albeit not to the extent as the sodium oxalate crystals. The sulfur particles would also aid the growth in the structure as they had with the NaCl structure, as explained earlier. As demonstrated in Keller's work [24] for clay particles in NaCl solution, NaCl follows a rock salt configuration therefore the structures obtained with NaCl salt solutions tend to have branches at 90°. This effect of the salt structure on the sulfur particles self-assembled structure has been confirmed again in case of the hydrochloric acid-thiosulphate reaction. Here too the resultant salt is NaCl and here as instead of bulky clay particles used in Keller's work we have nano to colloidal range sulfur particles. This leads to a much finer and much clearly defined grid-like labyrinthine structure than which was obtained in Keller's experiments, but the almost 90° branches formed in the presence of NaCl in both cases is unmistakable. With sulfuric acid the resultant structure is similar to the tree structure obtained for oxalic acid but it's different in the sense that it has spikier and more angular and rough branches. Additionally, as the production of sulfur particles is faster with sulfuric acid as compared to oxalic acid, the growth rate of branches is accelerated here which leads to increased branching and rougher edges of the branches.

3.3.4 Numerical modeling

Numerical modeling of the forces acting between particles, from an electrostatic standpoint can be done [2].

The surface potential of the particles (ψ_p) can be related to the surface charge density (σ_p) by the Gouy-Chapman relation:

$$\boldsymbol{\sigma_p = \frac{2\varepsilon\varepsilon_0 k_B T}{e\kappa^{-1}} \sinh\left(\frac{e\psi_p}{2k_B T}\right)} \qquad \textbf{(4)}$$

, where $\varepsilon\varepsilon_0$ = total permittivity of water, k_B = Boltzmann constant, T = ambient temperature (here 298 K), e = electronic unit charge, and κ^{-1} = Debye length. The electrostatic force between particle and substrate is calculated as:

$$\boldsymbol{F_{el}} = -\frac{\boldsymbol{128\pi d_p \gamma_s \gamma_p n k_B T \kappa^{-1}}}{\boldsymbol{2}} \boldsymbol{exp}\left(\frac{\boldsymbol{-z}}{\boldsymbol{\kappa^{-1}}}\right) \boldsymbol{n_z} \quad (\mathbf{5})$$
$$= \boldsymbol{a\, exp(-z/\kappa^{-1})}$$

, where d_p = particle diameter, n = number concentration of counter-ions, T = ambient temperature, κ^{-1} = Debye length, z = distance between particle and substrate, and n_z = unit vector normal to substrate. γ_p and γ_s are the functions of surface potentials (ψ_p and ψ_s) respectively.

$$\boldsymbol{\gamma_p = tanh\left(\frac{e\psi_p}{4k_B T}\right), \gamma_s = tanh\left(\frac{e\psi_s}{4k_B T}\right)} \quad (\mathbf{6})$$

The Debye screening length κ^{-1}, i.e. the thickness of diffuse electric double layer is given as:

$$\boldsymbol{\kappa^{-1}} = \sqrt{\frac{\boldsymbol{\varepsilon\varepsilon_0 k_B T}}{\boldsymbol{2N_A e^2 I}}} \quad (\mathbf{7})$$

, where N_A = Avogadro no., and I = ionic strength of the electrolyte salt used = $\boldsymbol{\frac{1}{2}\sum_{i=0}^{n} Z_i^2 C_i}$, where Z_i = valence of ions, and C_i = concentration of dissolved ions. The van der Waals attraction between substrate and particle is formulated as:

$$\boldsymbol{F_{vdw}} = \boldsymbol{\frac{1}{12} A d_p^3 \frac{\alpha_{rtd}}{z^2(z+d_p)^2} n_z} \quad (1)$$

, where A = Hamaker constant, and α_{rtd} = retardation factor for van der Waals force, which depends on the distance between particle and substrate*. Total DLVO force between particle and substrate is therefore:

$$\boldsymbol{F_{DLVO}} = \boldsymbol{F_{el} + F_{vdw}} \quad (\mathbf{9})$$

The numerical modeling is based on a finite-element code for droplet impact and heat transfer. This model has been validated for studies involving impact and heat transfer of molten metal and water drops, and for the evaporation of drops containing colloidal particles. Axisymmetric and laminar flow inside the drop has been assumed. Lagrangian framework

has been used for expressing the equations, since it provides precise modeling of free surface deformations and Laplace stresses. The use of a Lagrangian scheme where the nodes move with the fluid allows precise handling of free surface stresses and the full treatment of both convection and conduction heat transfer by solving the heat equation. Modeling of the evaporative flux along the drop-air interface, thermocapillary stresses, Marangoni flow, and wetting line motion can be done with the help of the numerical code. In addition, the code's dual time-step scheme can handle multiple time scales, ranging from nanoseconds for liquid-air interfacial capillary waves, to several seconds for the entire evaporation process [3]. Tracking of particle motion is done by solving an advection-diffusion equation for the particle concentration, and buoyancy is neglected. Interaction of the free surface of the drop with the growing deposit can be modeled using wetting angles criteria to predict the liquid drop's detachment from the ring, also known as depinning. Published results show unexpectedly small Marangoni convection in aqueous drops, Marangoni convection is not considered in the simulations presented here. In this paper, our numerical modeling is extended to consider the attractive DLVO force between the colloidal particles and the substrate, as follows. The governing equation for the particles transport is given by:

$$\frac{\partial X}{\partial t} + \nabla.(Xv) = D_{pl}\nabla^2 X \qquad (2)$$

, where X = concentration of particles, and D_{pl} = diffusion coefficient of particles in the drop liquid. The advection velocity is $v = v_{fluid} + v_{DLVO}$, where v_{fluid} = hydrodynamic velocity of fluid, and $v_{DLVO} = -\frac{2F_{DLVO+}}{6\pi\mu d_p}\boldsymbol{n_z}$.

CHAPTER 4

SELF-ASSEMBLY OF SODIUM CARBOXYMETHYLCELLULOSE AND STARCH ON GLASS SURFACE FROM EVAPORATING DROPS

4. SELF-ASSEMBLY OF SODIUM CARBOXYMETHYL CELLULOSE AND STARCH ON GLASS SURFACE FROM EVAPORATING DROPS

4.1 Introduction

In the current work, we studied the self-assembly of natural polymers like sodium carboxymethylcellulose in the presence of alkali medium and the effect of various reaction and drying parameters on the self-assembly. Fractal dimension of the structures is also calculated using special image processing software utilizing the box counting approach. Sodium carboxymethylcellulose is an anionic derivative of cellulose and is available in powder form. Previous research has been carried out on polyelectrolyte complexes consisting of CMCNa [25]. However, in this work, the interaction of CMCNa with alkali medium and its effect on self-assembly is being studied. Moreover, using different reaction parameters, we can study the overall effect of external factors on self-assembly. Also, from FTIR studies we can predict the formation of certain functional groups that are instrumental in the formation of various structures by self-assembly.

4.2 Materials and Methods

Chemicals used in this experiment were: sodium carboxymethylcellulose (CMCNa), sodium hydroxide (NaOH) 99% purity, and starch all from Merck India. Some of the apparatus used were glass slides, magnetic stirrer, ultrasonic homogenizer and drying oven. Ultrapure water having resistivity 18 MΩ cm and pH 6.4-6.5 was used for all experiments. 0.1 wt% CMCNa solution is prepared from 0.5 wt% stock. NaOH stock was prepared in advance and used through the experiments. Different concentrations of NaOH are prepared from the stock solution and the structure was observed at different pH by controlling the concentration of NaOH in the reaction mixture. Glass slides were initially washed with methanol and acetone to remove dirt and stains and then with deionized water and dried in hot air oven to remove existent moisture. Precursors were stirred for 20 min to achieve reaction equilibrium. If agglomerates are detected, the suspension was sonicated in ultrasonic equipment. Microliter drops of the suspension were put on glass slides using Hamilton

syringe, then the slides were dried using drying oven for 3 hours. The resulting dried drops were observed under an optical microscope (Hund, D600).

4.3 Results and Discussion

4.3.1 Observation of self-assembly

The self-assembly of sodium carboxymethyl cellulose in the presence of alkaline medium was studied under optical microscope. The drying time for the experiments was kept constant at 3 hours. The drops were put on a moisture-free glass slide in volumes of 10 and 20 µl using a Hamilton syringe.

4.3.2 Effect of pH

The structures at different pH were studied. pH was varied by varying the NaOH concentration. A concentration vs. pH curve was plotted to get an idea about the structure variation with pH.

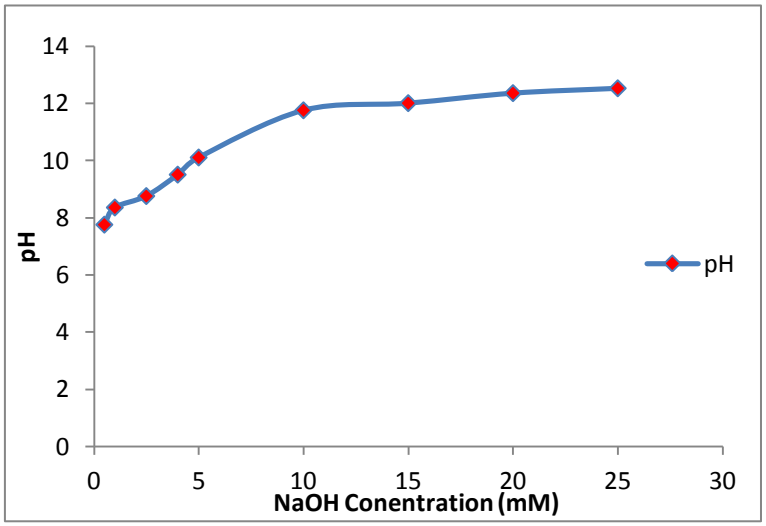

Figure 7 pH vs. concentration graph for CMCNa-NaOH-water system

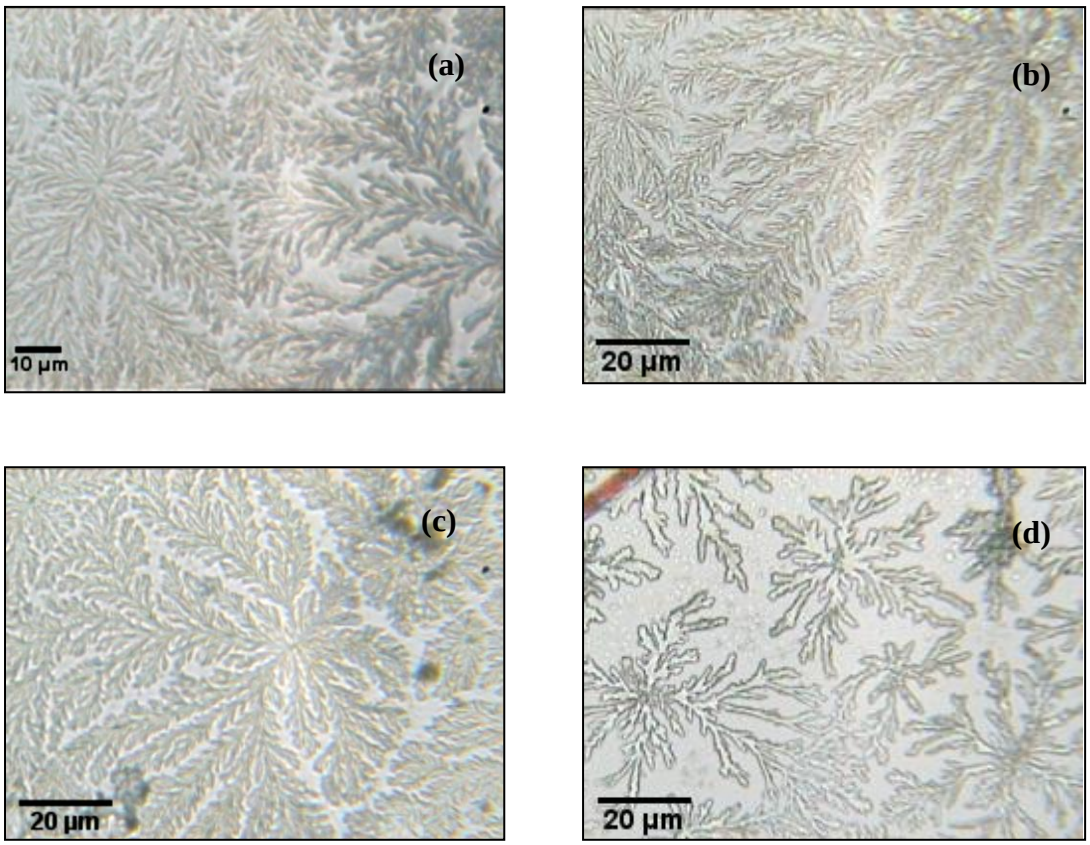

Figure 8 Fractal patterns formed at (a) pH=9.5, (b) pH=10, (c) pH = 12, (d) pH = 12.5

From the images it is clear that with increasing pH, the branches of fractal tree patterns increase in thickness. pH has a direct relationship with NaOH concentration in the mixture, and the increase in branch thickness can be attributed to this relationship. Also, with increase in pH, the protonation tendency decreases while zeta potential increases leading to fractal patterns [26].

4.3.3 Effect of drop volume

Drop volume was varied between 10 and 20 µl and the corresponding effects on self-assembly were studied. A clear-cut comparison between the patterns can be derived from the images.

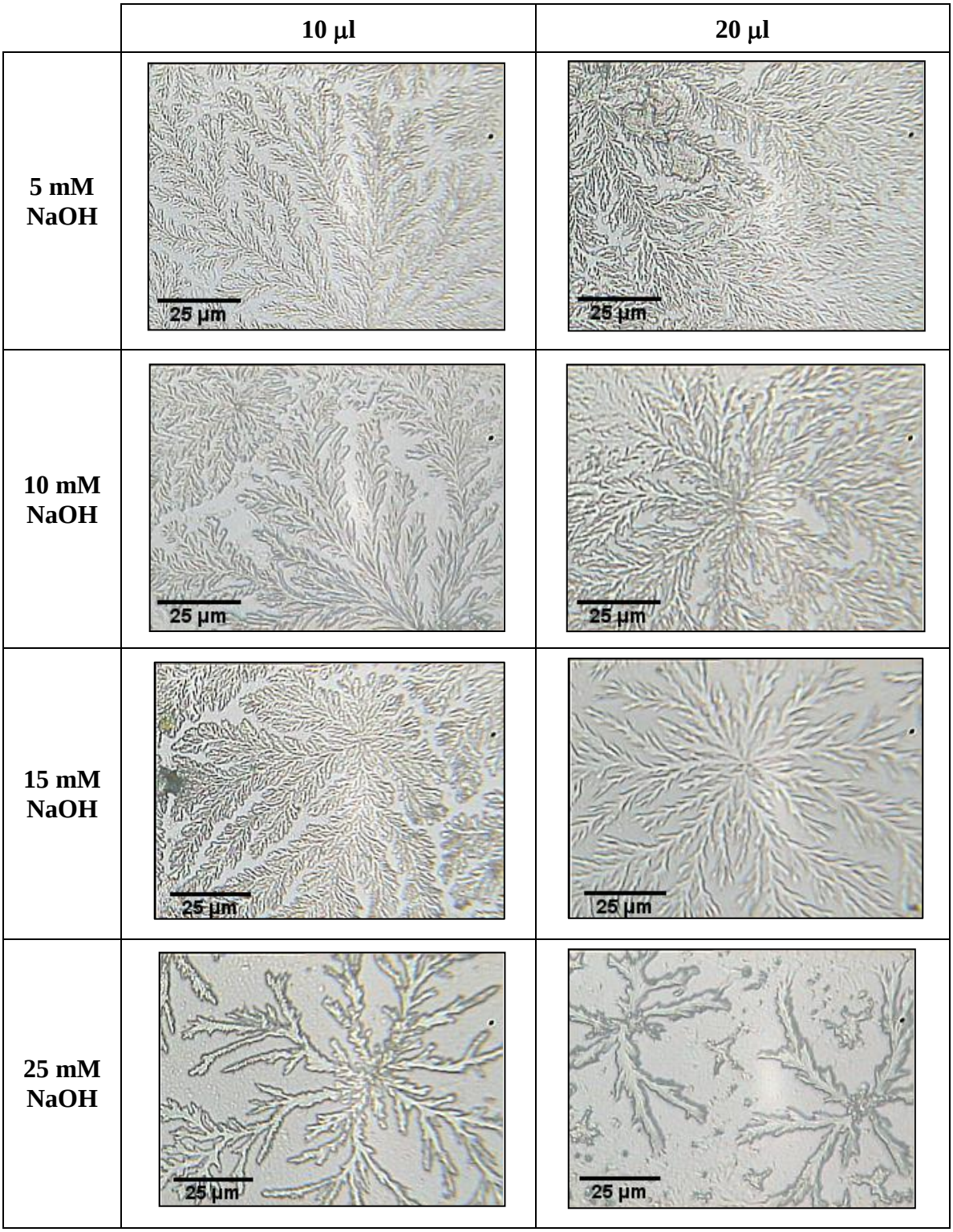

Figure 9 Fractal pattern formation at different NaOH concentrations (5, 10, 15, and 25 mM) and drop volume (10 and 20 µl) with 0.1 wt% CMCNa

When drop volume is high, the surface area increases thereby increasing the rate of evaporation from the drop. Since the contact area is large, surface forces are higher in

magnitude. Crystals formed are bigger in size due to higher rate of evaporation and hence the thickness of branches in the pattern increases. With increase in drop volume, particles get more time to settle down from their initial positions hence there is more deposition than lower drop volumes.

4.3.4 Effect of reaction temperature

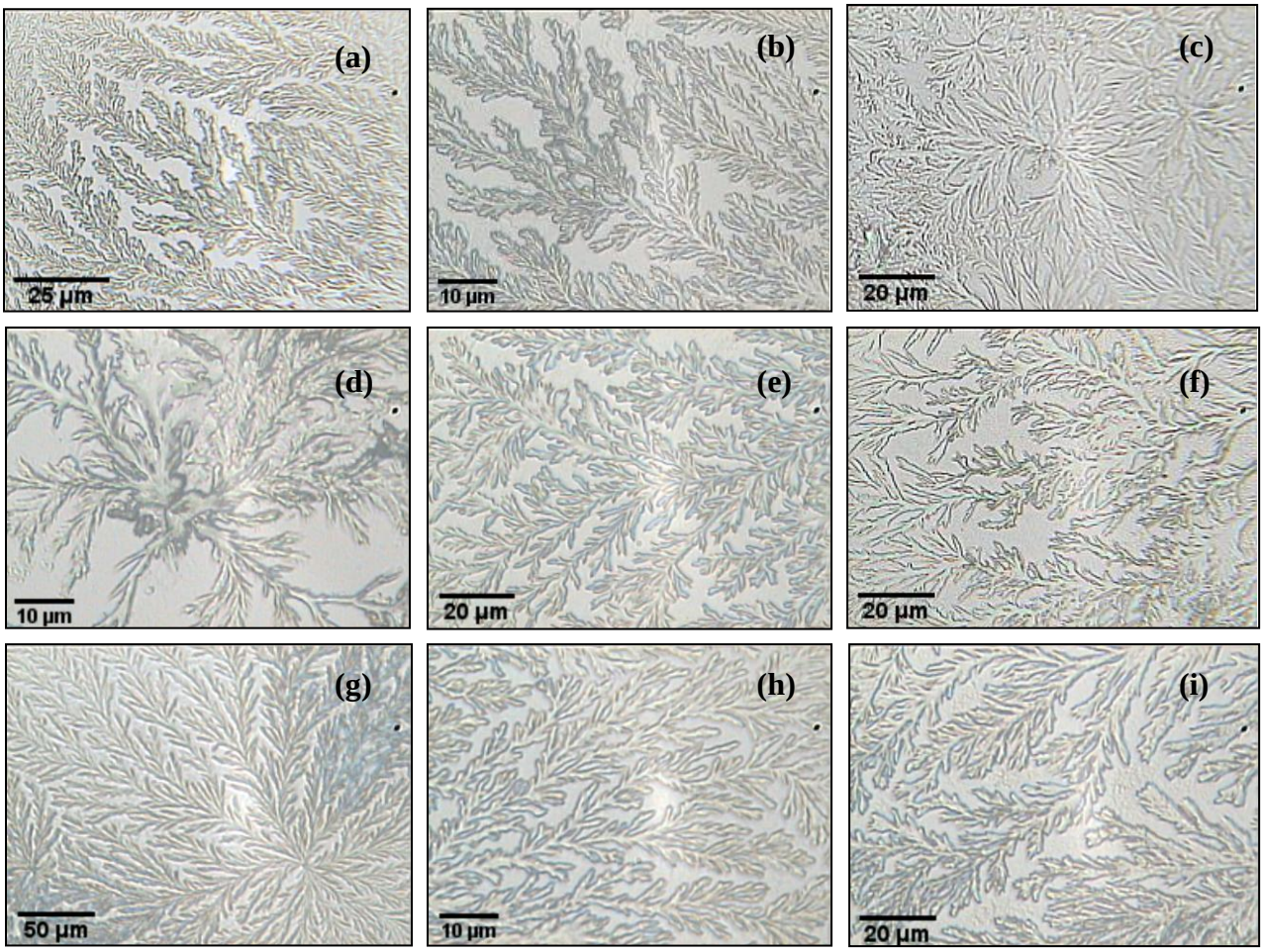

Figure 10 Pattern formation at different temperatures: T=10°C – (a),(b) pH=10, 25x and 40x magnification, (c),(d) pH=12, 25x and 40x magnification; T=70°C – (e) pH=10, (f) pH=12; T=50°C - (g),(h) pH=10, 10x and 40x magnification, (i) pH=12

The effect of reaction temperature on structure formation was studied at three different temperatures: 10°C, 50°C, and 70°C and two pHs: 10 and 12. It is clear from the images that at low temperatures, the angle between adjacent branches is small, while at high temperatures

crystal formation takes place which causes the branches to secede further apart. At intermediate temperatures, the branches are thicker and there is slight crystal formation too.

4.3.5 Self assembly of starch

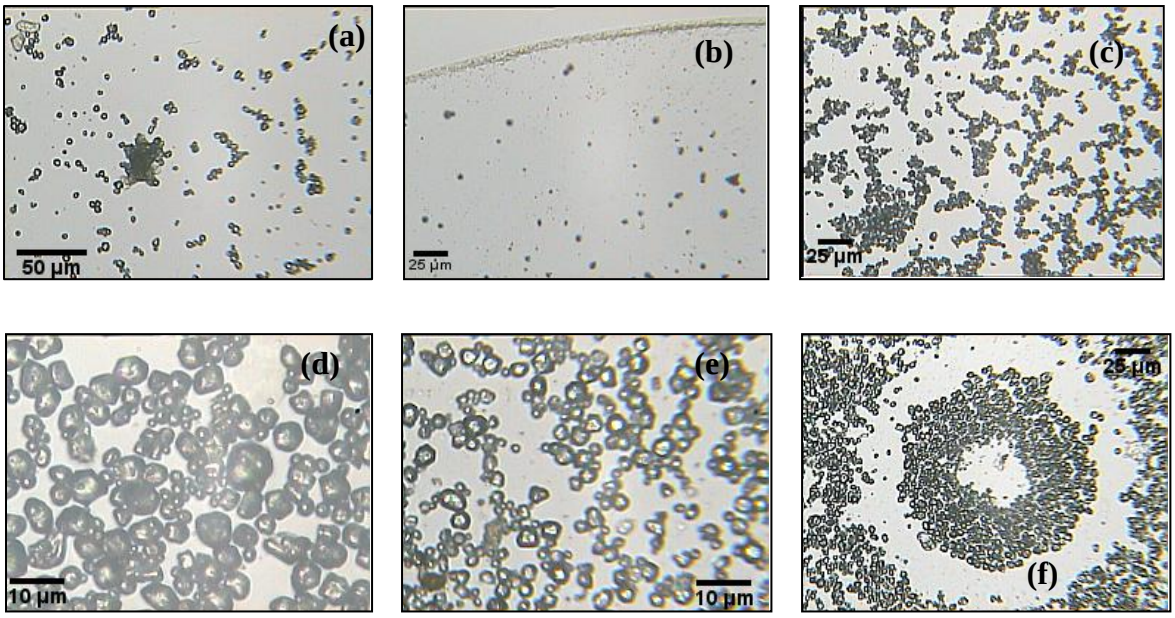

Figure 11 Self-assembly structures obtained using starch solutions: (a) 0.1 wt%, (b) 0.05 wt%, (c) 0.3 wt%, (d) 0.5 wt%, (e) 0.3 wt% with 5mM NaOH, and (f) 0.4 wt% with 5mM NaOH.

Starch consists of multiple glucose units joined together by glycosidic chains. In nature, starch molecules arrange themselves in semi-crystalline granules of definite size. Since these granules are micron sized, the forces of Vander Waals attraction and repulsion are not balanced, hence they tend to aggregate. This leads to disorderness in the system and this is the reason why no self-assembly is observed at room temperature. With the addition of NaOH, the granules become polarized to some extent, and rings are formed as can be seen in Fig. 11f.

4.3.6 FTIR analysis

FTIR analysis of pure CMCNa and CMCNa-NaOH solution were done. The FTIR analysis shows some characteristic peaks which provide information about the radicals present in pure CMCNa and those that are formed upon reaction of CMCNa and NaOH.

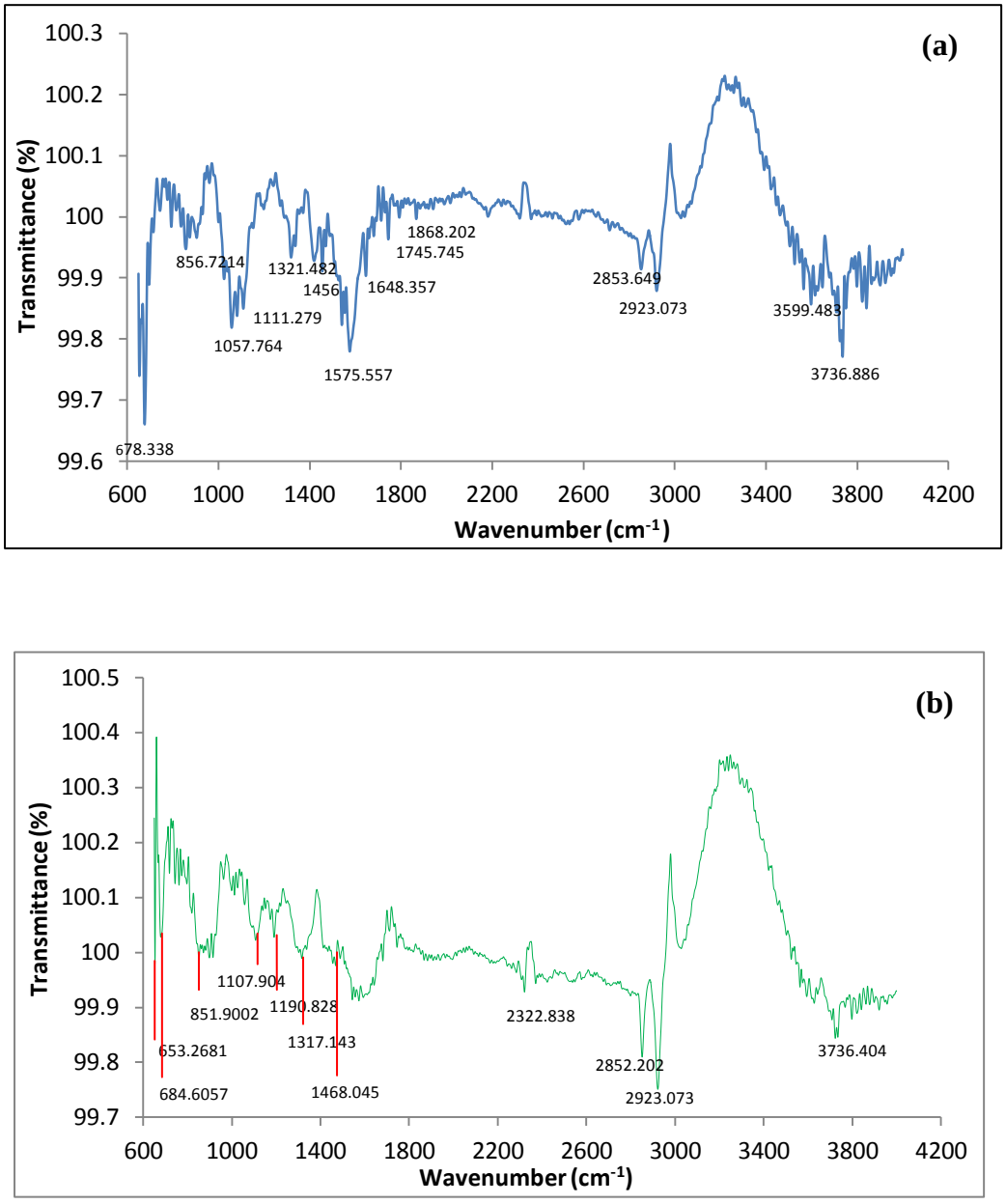

Figure 12 FTIR graphs for (a) pure CMCNa (b) CMCNa-NaOH system

Functional groups present are shown in the table below:

Functional group	Wavenumber (cm^{-1})
Carboxylate ion ($-CH_2COO^-$)	1550-1610
Carbonyl group (-C=O) stretch	1670-1820
Hydroxyl group (-O-H) stretch	3200-3600
Alkyl group (-C-H) stretch	2850-3000
Ether group (-O-) stretch	1000-1300
Carboxyl –OH stretch	2500-3000
Methyl group ($-CH_2$) scissoring	1420
-OH bending	1320

More specific analysis such as GC-MS (gas chromatography-mass spectroscopy) needs to be done to get a better idea about the reaction mechanism.

4.3.7 SEM analysis

SEM analysis of CMCNa with NaOH was done and it revealed the following results:

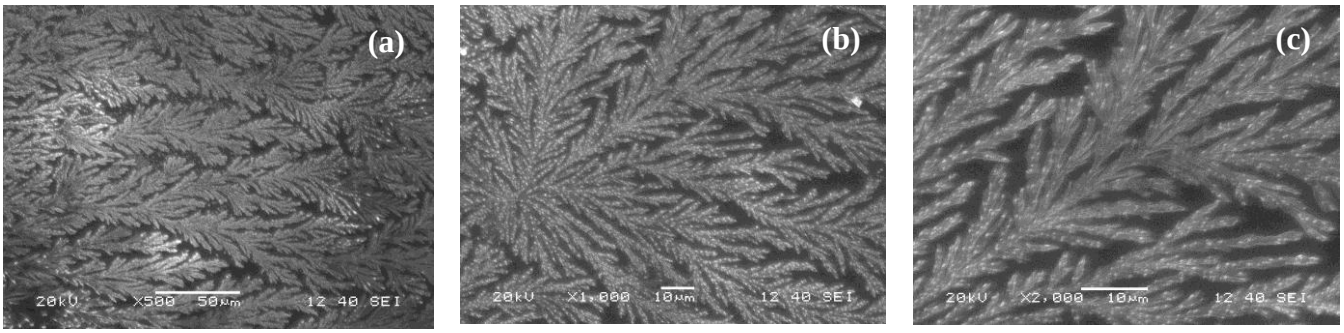

Figure 13 SEM micrographs of 0.1 wt% CMCNa with 5mM NaOH at different magnifications, (a) 500x, (b) 1000x, (c) 2000x

From the SEM images, it is observed that the fractal patterns obtained are crystalline in nature. Also, from EDS analysis of SEM, it is clear that the composition of carbon and sodium is high in the structures.

4.3.8 Fractal dimension

Fractal dimension is an index for analyzing fractal patterns by expressing their convolution as a ratio of the change in detail to the change in scale. In case of self-assembly, fractal dimension gives an idea about the complexity of the structure obtained and its effectiveness in terms of surface area covered. Fractal dimension is calculated by box-counting method, in which the image is divided into a no. of boxes of a fixed size so that it covers the smallest possible fractal element and analyzing each box iteratively to get the overall dimension. Fractal dimension was calculated by fractal3 version 3.4.7 software developed by NILGS, NARO. Box-counting method was employed to verify whether the structures are fractal or not. The variation of fractal dimension with NaOH concentration and temperature is shown below:

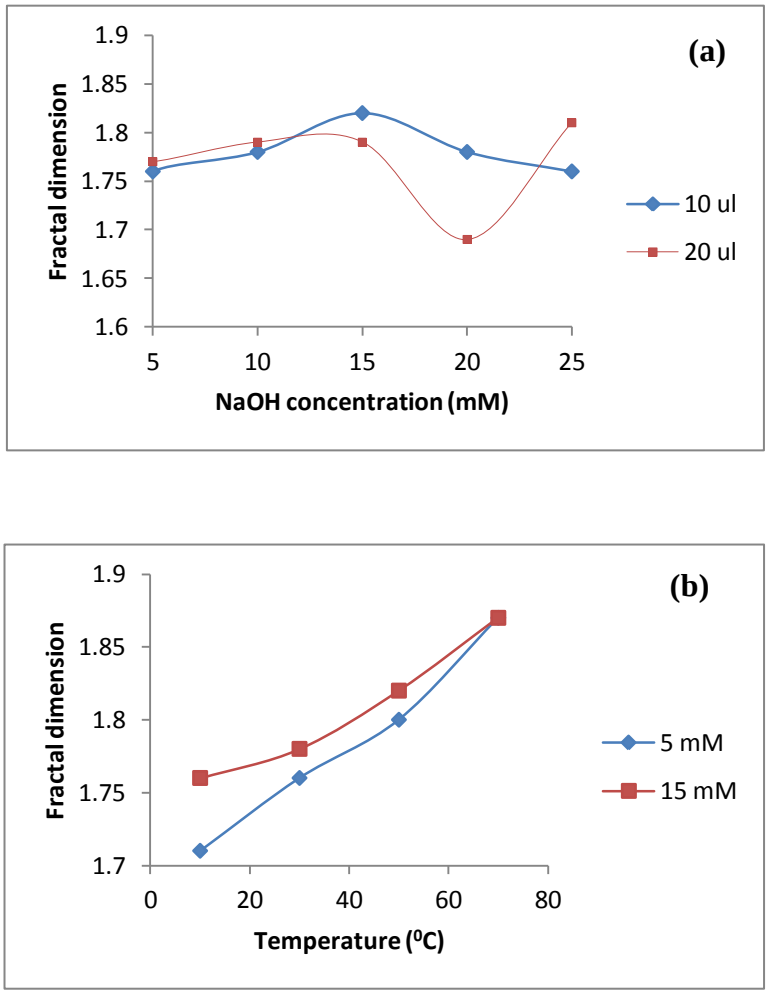

Figure 14 Fractal dimension variation with (a) NaOH concentration (b) temperature

CHAPTER 5

Conclusion

5. CONCLUSION

A distinct tree-like self-assembled structure with proper branches and stems can be formed on a hydrophilic glass surface using colloidal sulfur particles synthesized by oxalic acid catalyzed reaction of sodium thiosulphate. The structure is formed during the evaporation of liquid drop on the solid surface mainly because of the crystallization of sodium oxalate salt and the interplay of evaporative liquid flux and Marangoni flow inside the drop, capillary and van der Waals attractive forces between the particles. Similar sized sulfur particles alone dispersed in pure water cannot form tree-like structure, but sodium oxalate salt assists the sulfur particles to form the particular pattern. Some parameters such as particle size, particle and salt concentration, drop volume, acid to thiosulphate ratio, reaction time are very important for the formation of self-assembled structure from colloidal sulfur. The optimum particle size, particles and salt concentration, is very important for the formation of a proper structure. When the particle size and concentration is low less dense structure with more branches but less stems is formed.

The variation of salt concentration resulted in the structure surface transforming from smooth to rough as the salt concentration was changed from low to high. two different tree-like self-assembled structures with proper branches and stems and an interesting grid like structure with branches growing at almost 90° to the stems have been observed. They can be formed on a hydrophilic glass surface using colloidal sulfur particles synthesized by oxalic, sulfuric, and hydrochloric acid catalyzed reaction of sodium thiosulphate respectively. The structure is formed during the evaporation of liquid drop on the solid surface mainly because of the interplay of evaporative liquid flux and Marangoni flow inside the drop, capillary and van der Waals attractive forces between the particles; all of which influence the dendritic crystallization caused due to the presence of the respective salts, which in the end give each structure its unique form. An optimum particle concentration and size is very important for the formation of a proper structure. Generally when the particle size and concentration is low, less dense structure with more branches but fewer stems is formed. This study demonstrates a facile method as to how a simple one pot method can be used to exploit the crystalline nature of the salts so commonly generated in many reactions. Moreover, the usage of the in-situ generated sulfur particles effectively enhances the pattern formation process and it also shows how different patterns can be generated using the combination of self-assembly techniques and dendritic crystallization.

Sodium CMC showed some interesting fractal patterns with NaOH. At very low NaOH concentrations (0.5 - 2.5 mM), banana leaf like structures were observed with thick 90^0 branches. Pattern formation is at its premature stage and the morphology of the patterns depicts it. At medium NaOH concentration (4 - 15mM), pattern formation is optimum and we get fractal trees with optimum fractal dimensions as is clear from the graphs. At high NaOH concentration (20-25 mM), thicker fractal or floral (flower-like) patterns are formed. With increase in NaOH concentration, pH increases. Since NaOH is a strong electrolyte, it dissociates into Na^+ and OH^- ions and causes the water molecule to dissociate into H^+ and OH^-. The H^+ ion causes protonation of the COONa groups on the CMCNa molecule and generates an energy barrier between adjacent branches [26]. The separation of branches leads to fractal patterns. With decreasing pH, the protonation tendency decreases and energy barrier decreases, causing branches to converge and thicken in size due to continuous deposition. At high pH, the accumulation is higher and it dominates the effect of energy barrier. The structure variation with mixing of temperature can be attributed to the change in entropy [27]. It is pretty obvious that there is hydrogen bonding interaction at specific polymer sites. The hydrogen bonds start to break at high temperatures while at low temperatures entropy is reduced and crystallinity is developed. At high temperatures, thicker structures are formed with lesser fractality than the structures obtained at lower temperatures.

Fractal patterns are ideal for fabrication of nano-circuits and for surface-active catalysts. Fractal dimension is significant for the determination of effective surface area of thin films which has importance in photoelectronics. Self-assembly in polyelectrolyte systems is garnering importance nowadays due to the intricate patterns formed [38]. Several complex substances found in nature such as cellulose are known to form self-assembled structures with polyelectrolytes [25].

CHAPTER 6

Future Work

6. FUTURE WORK

This work can be further extended and deeply explored. There is virtually no limitation to raw materials that can be used for self-assembly and fabrication of functionalized structures and new materials. In the future the following work can be done:

1. Effect of surface property on self-assembly can be studied by the use of different varieties of surfactants adsorbed on hydrophilic glass slides.
2. Similar self-assemblies can be tried with other materials as the mobile components, such as polystyrene microspheres, glass microbeads, titania nanoparticles and so on.
3. Different solvents may also show variation in the structures.
4. More crystalline and semi-crystalline materials can be explored to assist and enhance the structure forming abilities of the particles.
5. More detailed studies using goniometry (OCA measurement) and AFM instruments can be done. This will help to generate drying patterns and drop stain texture and topology data.
6. The structures can be functionalized with other materials as per the requirement or application.

References

REFERENCES

1. Deegan, R.D., Bakajin, O., Dupont, T.F., 1997. Capillary flow as the cause of ring stains from
dried liquid drops. Nature 827-829.

2. Banerjee, R., Hazra, S., Banerjee, S., Sanyal, M., 2009. Nanopattern formation in self-assembled monolayers of thiol-capped Au nanocrystals. Phys. Rev. E 80, 1-9..

3. Bhardwaj, R., Fang, X., Somasundaran, P., Attinger, D., 2010. Self-assembly of colloidal particles from evaporating droplets: role of DLVO interactions and proposition of a phase diagram. Langmuir 26, 7833-7842.

4. Sommer, A.P., Ben-Moshe, M., Magdassi, S., 2004. Size-Discriminative Self-Assembly of Nanospheres in Evaporating Drops. J. Phys. Chem. B 108, 8-10.

5. Shen, X., Ho, C.-M., Wong, T.-S., 2010. Minimal size of coffee ring structure. J. Phys. Chem. B 114, 5269-5274.

6. Eral, H.B., Augustine, D.M., Duits, M.H.G., Mugele, F., 2011. Suppressing the coffee stain effect: how to control colloidal self-assembly in evaporating drops using electrowetting. Soft Matter 7, 4954-4958.

7. Lao, J.Y., Wen, J.G., Ren, Z.F., 2002. Hierarchical ZnO Nanostructures. Nano Letters 2, 1287- 1291.

8. Whitesides, G.M., Grzybowski, B., 2002. Self-assembly at all scales. Science 295, 2418-2421.

Whitesides, G.M., Lipomi, D.J., 2009. Soft nanotechnology: “structure”vs.“function”. Farad. Discuss. 143, 373-384.

9. Breen, T.L., 1999. Design and Self-Assembly of Open, Regular, 3D Mesostructures. Science 284, 948-951.

10. Gracias, D.H., 2000. Forming Electrical Networks in Three Dimensions by Self-Assembly. Science 289, 1170-1172.

11. Cheng, C., Liu, B., Yang, H., Zhou, W., Sun, L., Chen, R., Yu, S.F., Zhang, J., Gong, H., Sun, H., Fan, H.J., 2009. Hierarchical assembly of ZnO nanostructures on SnO(2) backbone nanowires: low-temperature hydrothermal preparation and optical properties. ACS Nano 3, 3069-3076.

12. Yang, Y., Wang, C., 2009. Solvent effects on two-dimensional molecular self-assemblies investigated by using scanning tunneling microscopy. Curr. Opin. Colloid Interface Sci. 14, 135-147.
13. Cho, Y.-S., Yi, G.-R., Lim, J.-M., Kim, S.-H., Manoharan, V.N., Pine, D.J., Yang, S.-M., 2005. Self-organization of bidisperse colloids in water droplets. J. Am. Chem. Soc. 127, 15968-
15975.
14. Park, J., Moon, J., 2006. Control of colloidal particle deposit patterns within picoliter droplets ejected by ink-jet printing. Langmuir 22, 3506-3513.
15. John, N.S., Raina, G., Sharma, A., Kulkarni, G.U., 2010. Cellular network formation of hydrophobic alkanethiol capped gold nanoparticles on mica surface mediated by water islands. J. Chem. Phys. 133, 094704.
16. Jun, Y.-wook, Lee, J.-H., Choi, J.-sil, Cheon, J., 2005. Symmetry-controlled colloidal nanocrystals: nonhydrolytic chemical synthesis and shape determining parameters. J. Phys. Chem. B 109, 14795-806.
17. Nagayama, K., 1994. Formation of two dimensional colloidal crystals in liquid films under the action of capillary forces. J. Phys.: Condens. Matter 6, 395-402.
18. Kralchevsky, P.A., Denkov, N.D., 2001. Capillary forces and structuring in layers of colloid particles. Curr. Opin. Colloid Interface Sci. 6, 383–401.
19. Vancea, I., Thiele, U., Pauliac-Vaujour, E., Stannard, A., Martin, C., Blunt, M., Moriarty, P., 2008. Front instabilities in evaporatively dewetting nanofluids. Phys. Rev. E 78, 014601-
014615.
20. Witten, T., Sander, L., 1981. Diffusion-Limited Aggregation, a Kinetic Critical Phenomenon. Phys. Rev. Lett. 47, 1400-1403.
21. Johnson, B., Sekerka, R., 1995. Diffusion-limited aggregation: Connection to a free-boundary problem and lattice anisotropy. Phys. Rev. E 52, 6404-6414.
22. Mullins, W.W., Sekerka, R.F., 1963. Morphological Stability of a Particle Growing by Diffusion or Heat Flow. J. Appl. Phys. 34, 323-329.
23. Ghosh Chaudhuri, R., Paria, S., 2009. Dynamic contact angles on PTFE surface by aqueous surfactant solution in the absence and presence of electrolytes. J. Colloid Interface Sci. 337, 555
24. Keller, W., 1988. Morphology of clay deposited by evaporation of visually clear aqueous phases from clay-water suspensions. Appl. Clay Sci. 3, 101-110.

25. Kotz, J., Kosmella, S., Beitz, T., “Self-assembled polyelectrolyte systems”, Prog. Polym. Sci. (2001) 1199-1232

26. Zhao, Q., An, Q., Qian, J., Wang, X., Zhou, Y., “Insight into Fractal Self-Assembly of Poly(diallyldimethylammonium chloride)/Sodium Carboxymethyl Cellulose Polyelectrolyte Complex Nanoparticles”, J. Phys. Chem., 2011, 115, 14601-14911

27. Dimitrov, I., Trzebicka, B., Muler, A.H.E., Dworak, A., Tsvetanov, C.B., “Thermosensitive water-soluble copolymers with doubly responsive reversibly interacting entities”, Prog. Polym. Sci. 32 (2007) 1275–1343

28. Kaya, D., Belyi, V.A., Muthukumar, M., 2010. Pattern formation in drying droplets of polyelectrolyte and salt. J. Chem. Phys. 133, 114905-114909.